Chapter 4

Competition indices as a measure for individual wind loading

Abstract

The wind loading experienced by a tree in a forest stand is influenced by its relative position in the stand. Most of the energy is absorbed in the upper parts of the forest canopy. Hence the dominant trees create a sheltered environment for the smaller ones.

Wind risk models like ForestGALES are at the moment not able to account for any differences in tree properties, because every tree in the stand is considered to have the same properties. With the advent of low impact silviculture systems, which create irregular stand structures, new approaches need to be found.

Simultaneous measurements of wind speed and turning moment were undertaken in an even-aged Sitka spruce plantation forest. The data are used to test the performance of several competition indices in explaining differences in wind loading between nine neighbouring trees.

Results show that the competition indices are able to explain a lot of the variance in wind loading, and indices with high input requirements do not perform better than the simpler ones. The data for two of the trees showed an increased turning moment, when the wind was blowing from a direction with lower competition. However, the amount of data was not sufficient for parametrisation of the impact of gaps.

4.1 Introduction

The drag a solitary tree has to withstand is a function of the wind profile, crown area, and drag coefficient. In a forest the relationship is affected by the presence of neighbouring trees which influence the wind profile and possibly increase the damping due to crown clashing (Rudnicki et al., 2003, 2008). Therefore a dominant tree has to withstand higher wind loading compared to a suppressed one, which benefits from the shelter provided by its taller neighbours. This is compensated for by higher stiffness and better root anchorage, which increase the resistance to wind damage (Nicoll and Ray, 1996).

This level of complexity is currently not accounted for in wind risk models, because wind-tree interactions are modelled at the stand level scale rather than at the individual tree scale (Gardiner et al., 2000). The models treat each tree in the same way assuming that their properties are equal. Hence every tree in the stand is exposed to the same drag, has the same critical turning moment and therefore the same risk of damage by the wind. As foresters in Britain are encouraged to manage more stands under low impact silvicultural systems, this will increase the number of irregular stands, and creates a demand for predicting the response of trees on an individual tree level (Rojo and Orois, 2005).

The hypothesis for this chapter is that competition indices are a suitable tool to predict wind loading at an individual tree level. Such indices are often used in growth models (Courbaud et al. (2001); Pretzsch et al. (2002); Stadt et al. (2007); Schröder et al. (2007)). A correlation between competition indices and wind loading would allow a straight forward linking of growth and wind risk models. At the same time it would allow the simulation of different forest management practises and their impact on the risk of wind damage. Following this, the approach could then be used to identify best management practise. This is of particular importance in Britain, where the transformation of regular into irregular stands is a major goal for forestry (Mason, 2002). This aim can only be achieved by creating a light regime at the forest floor, which allows the establishment of natural regeneration. Therefore thinning is inevitable, which at least in the short term can compromise the stability of the stand (Page et al., 2001; Hale et al., 2004).

4.2 Material and methods

4.2.1 Site characteristics

The field experiment was conducted from May until November 2005 in a pure Sitka spruce (*Picea sitchensis* (Bong.) Carr.) stand in Clocaenog Forest, North Wales (53°07′40″N, 3°42′96″W, 395 m a.s.l.). The stand was established as a row mixture of Sitka spruce and Scots pine (*Pinus sylvestris* L.) or lodgepole pine (*Pinus contorta* Dougl. ex Loud.) in 1951 and was thinned three times since (1975, 1993, and 1999).

Stand density was 292 trees ha^{-1} and basal area was 30.8 $m^2\,ha^{-1}$ (2002). The floor is amply covered by about 10 year old natural regeneration. The current state of the stand can be seen as starting point of a successful transformation towards an irregular stand structure (Schütz, 2001).

4.2.2 Tree characteristics

In total nine trees were chosen as experimental trees, which were arranged in a 3×3 array. Due to the maturity of the stand the nine trees differ widely regarding their properties. The height of the tallest tree (80: 31.9 m) exceeds the smallest one (42: 22.8 m) by more than 9 m. For each tree the crown radius was measured by going from the trunk to the crown edge at different angles. A stick was placed vertically beneath the crown edge. For each point the angle and distance to the trunk was measured. The average crown radius was calculated as the radius of a circle with the same area as the measured polygon. For the competition indices the neighbouring trees have to be defined. To do this the tree positions were used to create a Voronoi mosaic. Trees are considered as neighbours if they share the same side of one of the polygons. Table 4.1 lists the properties of the nine experimental trees as well as their neighbours.

Table 4.1: Mensurational and positional data for the nine experimental trees. Measurements were taken in 2005. (h: height, dbh: diameter at breast height, cr-rad: average crown radius, cr-class: crown class)

ID	h (m)	dbh (cm)	cr-rad (m)	neighbours (ID)	cr-class
4	29.6	59.8	4.2	[2,3,5,6,38,42]	dom
37	31.1	42.2	2.8	[36,38,39,77,79,80,502]	dom
38	27.3	38.9	2.9	[3,4,35,36,37,39,40,42]	co-dom
39	26.9	35.4	2.9	[37,38,40,41,80]	co-dom
40	28.0	37.6	2.5	[38,39,41,42,43]	co-dom
41	24.3	34.0	3.1	[39,40,43,46,80,83,84]	surp
42	22.8	28.5	2.1	[4,6,8,38,40,43,44,45]	surp
43	30.5	47.2	3.1	[40,41,42,45,46]	dom
80	31.9	54.5	3.6	[37,39,41,79,81,84,85]	dom

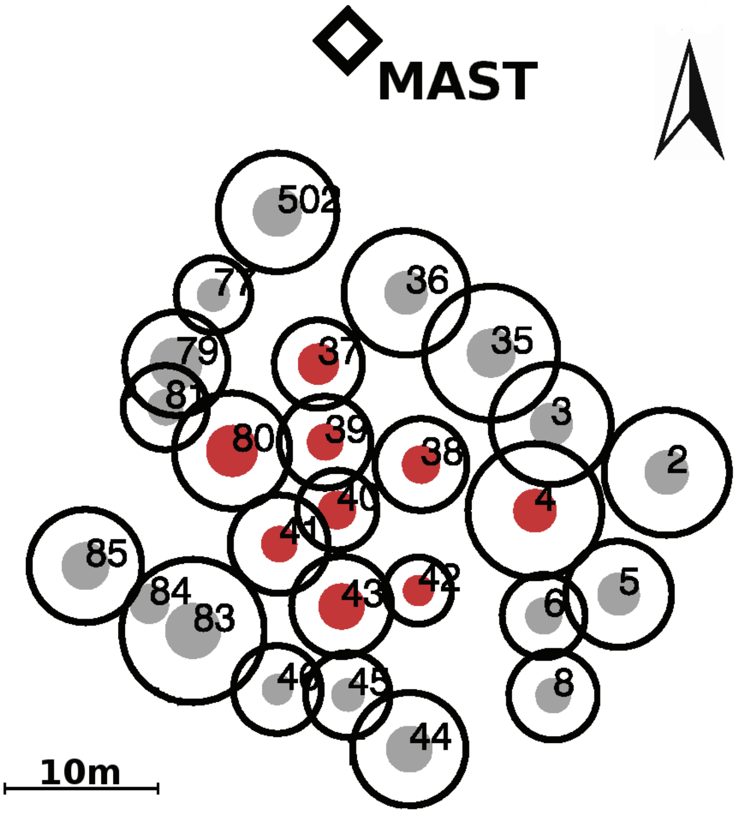

Figure 4.1: Map showing the nine experimental trees (red circles) and their direct neighbours (grey circles). The black circles represent the crown radii. Note that the meteorological mast was located inside the forest stand. Because the experimental trees were located at the edge of the plot, the coordinates of the trees around the mast are unknown.

4.2.3 Instrumentation

General

No mains was available at the site. Because the logging system was relatively power demanding, the decision was made that it would only be switched on when a gale event was expected. In total more than 400 hours of data were gathered between May and November 2005. The measured maximum hourly mean wind speed was 8.3 m s^{-1}. All available hourly data values are shown in Figure 4.2.

Wind measurements

A 30 m tall mast (TallTower, NRG Systems, US) was erected in the forest in proximity to the nine experimental trees (see Fig. 4.1). The mast was equipped

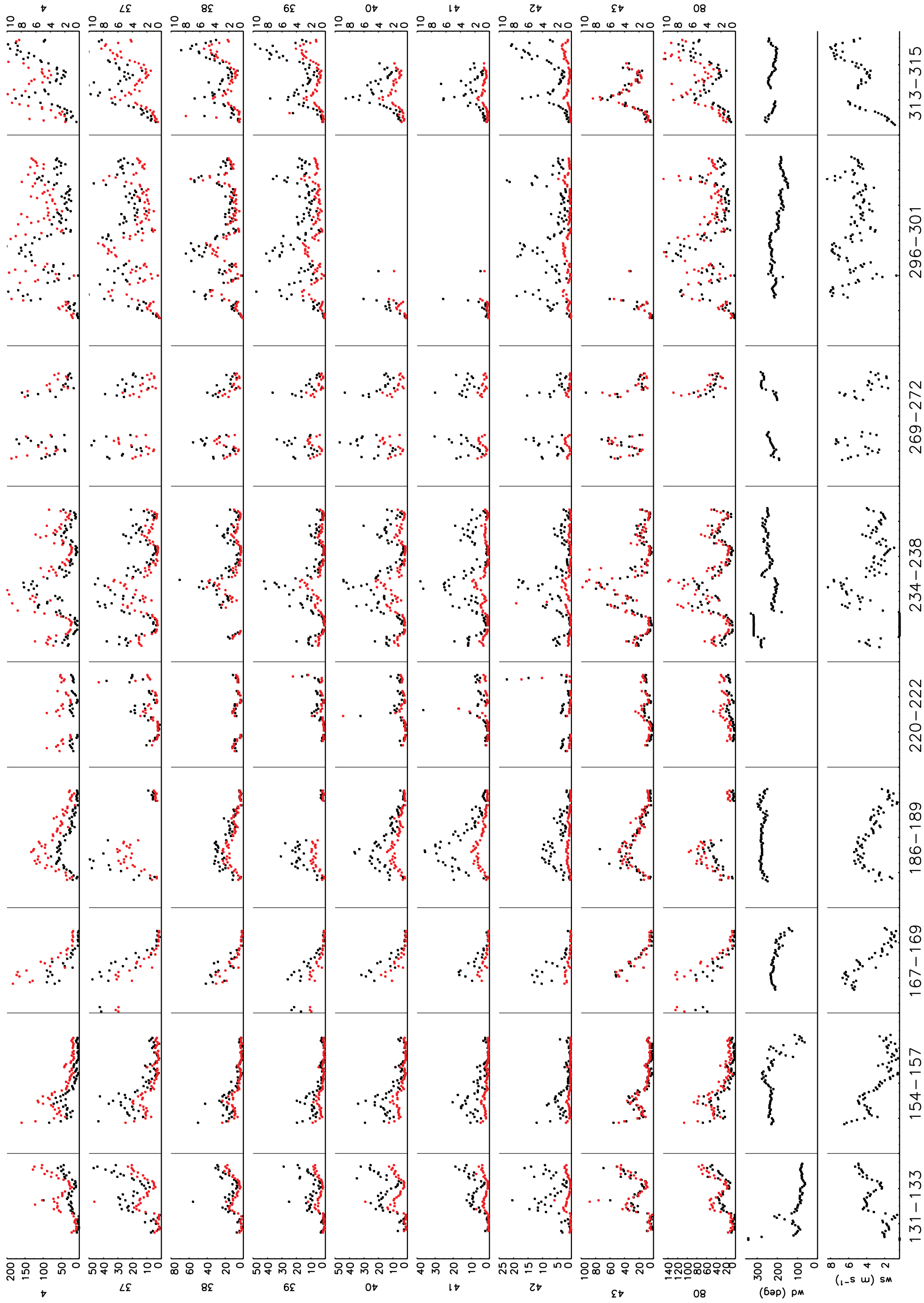

Figure 4.2: Time series of all available hourly maximum (y-axis on the left hand side, black dots) and mean (y-axis on the right hand side, red dots) turning moments in kNm for the nine experimental trees. The scaling of the ordinates varies between plots. The two bottom graphs are mean wind direction (wd) at 27.0 m and hourly mean wind speed at 30.8 m height (ws). The time series are not continuous. The numbers at the bottom indicate the julian day 2005 for each section separated by vertical lines.

with eight cup anemometers (heights (m): 5, 10, 15, 18, 21, 24, 27, 30.8; NRG#40, NRG Systems, US) and two wind vanes (heights (m): 15, 27; NRG#200P, NRG Systems, US). The four upper cup anemometers and the wind vanes were logged every 3 s using a 21X data logger (Campbell Scientific, Logan, US). The lower four cup anemometers were logged once a minute by another data logger (Holtech, Durham, UK).

Turning moments

The wind induced turning moments were measured on nine trees using strain transducers (Blackburn, 1997; Moore et al., 2005). Each experimental tree was equipped with two strain transducers, which were screwed orthogonally into the trunk at about 1.3 m height. To achieve sufficient resolution the two strain gauges of each transducer were incorporated into a Wheatstone bridge, which was completed with two precision resistors (348 Ω). The signal was measured using a differential channel of a CR10 data logger (Campbell Scientific, Logan, US) at 4 Hz. The data loggers were programmed to use an excitation of 2.5 V and to use the highest possible resolution (0.33 μV). All CR10s were part of a RS485 network. An industrial PC provided data storage, which stored all raw data as plain text files.

From the formulas by Moore and Maguire (2004) the eigenfrequencies of the nine experimental trees are calculated to be in the range 0.24 to 0.33 Hz (mean: 0.28 Hz). This means that a single sway circle is covered by about 16 measurements.

Tree bending causes a change in distance between the two points where the strain transducer is screwed into the trunk. The definition of strain is:

$$\varepsilon = \frac{\Delta L}{L} \tag{4.1}$$

where ΔL (m) is the change in distance and L (m) the total distance between the attachment points. The bending causes a change in electrical resistance of the active strain gauge, which can be measured as voltage across two legs of a Wheatstone bridge. The measured strain is linearly correlated to the wind induced turning moment. To be able to relate the strain signal to the turning moment it is necessary to calibrate each strain transducer individually by stepwise pulling of the experimental trees into two directions while measuring the applied force using a load cell (Model 616, Tedea Huntleigh, US). The applied turning moment is calculated as:

$$M = F \cdot cos(\alpha) \cdot h \tag{4.2}$$

where F (N) is the applied force measured by a load cell, α (°) the rope angle, and h (m) the height of the anchor point on the experimental tree. For all strain transducers a linear relationship between turning moment and signal output was measured. The slope of the regression line was used as calibration coefficient. For a more extensive description of the calibration procedure see Appendix A.

4.2.4 Turning moment coefficient

Drag (F_D) is defined as the force exerted by a fluid on an object and is calculated as:

$$F_D = \rho \cdot \int_0^z C_D(z) \cdot A(z) \cdot u(z)^2 \, dz \tag{4.3}$$

where ρ ($1.226\,\mathrm{kg\,m^{-3}}$) is air density, C_D ($-$) is the dimensionless drag coefficient, A ($\mathrm{m^2}$) is the projected crown area, u ($\mathrm{m\,s^{-1}}$) is the horizontal wind speed, and z (m) is height above ground. In contrast to buildings trees cannot be considered as rigid obstacles with a constant projected area. Trees streamline in the wind and therefore C_D and A themselves are functions of wind speed (Mayhead, 1973; Rudnicki et al., 2004). However, as a simplification of Equation 4.3 the drag can be described as a function of a reference wind speed where:

$$F_D \propto u^2 \tag{4.4}$$

If in a next step it is assumed that the drag acts as a point load then the drag is also proportional to the turning moment a tree experiences. Hence the turning moment is proportional to squared wind speed:

$$M \propto u^2 \tag{4.5}$$

The data from this field study show that the suggested relationship is valid for the wind speed range of the experiment. The simplifications allow us to calculate the **T**urning **M**oment **C**oefficient (TMC in kg) for each experimental tree, which is defined as fraction of experienced turning moment and squared wind speed at 30.8 m height:

$$TMC = \frac{M}{u^2_{30.8m}} \tag{4.6}$$

A graphical illustration of the TMC is the slope of the regression line of the measured turning moments plotted against the squared horizontal wind speed as it is shown in Figure 4.3.

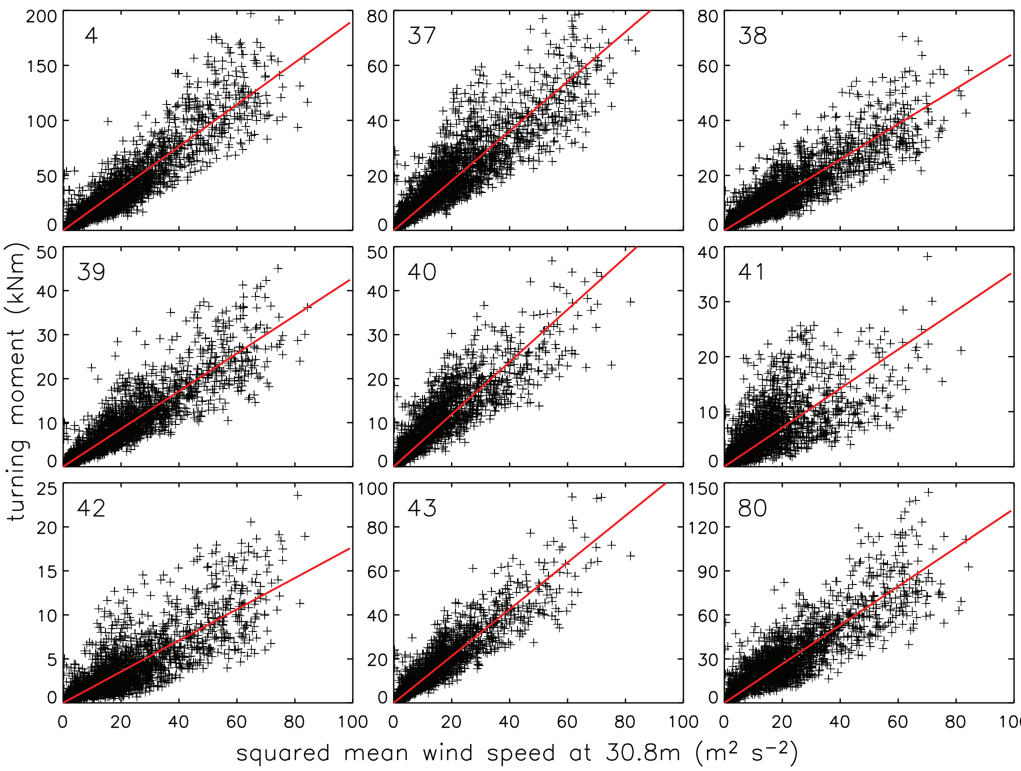

Figure 4.3: Maximum turning moments of 10 min time intervals plotted versus squared mean wind speed at 30.8 m. Note that the scales of the ordinate vary. The red lines are the best fit of a linear regression.

The calculated TMCs are listed in Table 4.2. Taller and therefore more exposed trees (ID: 4,37,43,80) have higher values than more suppressed trees.

Table 4.2: Turning moment coefficient (TMC), Pearson correlation coefficient (r), and number of data points used for the regression analysis.

ID	TMC (kg)	r	n
4	1.91	0.91	2338
37	0.90	0.88	2228
38	0.64	0.89	2295
39	0.43	0.89	2236
40	0.60	0.87	1798
41	0.35	0.68	1782
42	0.18	0.82	2336
43	1.06	0.91	1797
80	1.32	0.87	2146

4.2.5 Competition indices

Trees within a forest stand find themself in permanent competition for resources like light and nutrients. Availability of these resources has an impact on the photosynthetic rate, which itself governs biomass production and growth rate. Since dominant trees are more exposed to light and have increased total leaf area, they can photosynthesise more.

A coarse qualitative approach is the subdivision of the trees into four crown classes (1) dominant, (2) co-dominant, (3) subdominant, and (4) suppressed. A finer and non-discrete quantification can be achieved using distant dependent competition indices, which take the relation of tree properties of a subject tree and its neighbours into consideration. Many different indices have been developed, with differing data demands. A wide range of indices, which require just tree position and one additional tree characteristic (e.g. diameter at breast height, height), have been used and gave satisfying results for describing crown properties (e.g Rouvinen and Kuuluvainen, 1997). Good correlation has been found between competition indices and individual tree growth (e.g. Stadt et al., 2007; Mailly et al., 2003). Hence such approaches are often used as basis for growth simulators (e.g. Pretzsch et al., 2002).

For all the used indices a neighbour of the subject tree is defined as a tree, which shares a side of the Voronoi mosaic with the subject tree. Tree positions are used for the determination of the polygons (Aurenhammer and Klein, 2000).

h:dbh - slenderness

The height to diameter at breast height ratio (*h:dbh*) - also called slenderness - does not take tree position into account. Thus it is called a distance independent index. Several authors used the ratio at the stand level as a measure of stability (Wonn and O'Hara, 2001; Kenk and Guehne, 2001). Stands with lower ratios are regarded as more stable. Achim et al. (2005) used a similar approach to rate the stability of Canadian balsam fir (*Abies balsamea* (L.) Mill.) stands.

Indices by Rouvinen and Kuuluvainen, 1997

Rouvinen and Kuuluvainen (1997) compared the performance of several competition indices to describe crown properties of natural mature Scots pine trees in Finland. Here their indices numbered 10 to 12 are used, which are defined in the appendix of their article.

These three indices only require *dbh*, tree height of the neighbouring trees, and distance to the neighbours what makes these indices distance-dependant. The equations for the three indices are:

$$CI_{10} = \sum_{i=1}^{n} \frac{\frac{dbh_j}{dbh_i}}{dist_{ij}} \tag{4.7}$$

$$CI_{11} = \sum_{i=1}^{n} \frac{\frac{dbh_j}{dbh_i}}{{dist_{ij}}^2} \tag{4.8}$$

$$CI_{12} = \sum_{i=1}^{n} \frac{\left(\frac{dbh_j}{dbh_i}\right)^2}{dist_{ij}} \tag{4.9}$$

where *dbh* (m) is diameter at breast height, i and j represent neighbour and subject tree, respectively. $dist_{ij}$ (m) is the distance between subject and objective tree. The impact of all neighbours is accounted for by summing the individual values up over the number of neighbours (n).

Hegyi Index

The method of distant dependent competition indices was developed by Hegyi (1974). The formula we use here is:

$$CI_{\text{Hegyi}} = \sum_{i=1}^{n} \frac{\left(\frac{cr_j}{cr_i}\right)^{1.3}}{dist_{ij}^{\;0.4}} \tag{4.10}$$

where cr (m) is the average crown radius and $dist_{ij}$ (m) the horizontal distance between subject tree and competitor. The index is the sum of the values calculated for each neighbour.

Schütz-Index, 1989

Competition in mixed species stands is more complicated compared to monocultures, because the crown shape of the species differ. Schütz (1989) developed a competition index which uses crown dimension to take this into account. This index is the most demanding in terms of data requirements:

$$CI_{\text{Schütz}} = \sum_{i=1}^{n} 0.5 - \frac{dist_{ij} - (cr_j + cr_i)}{(cr_j + cr_i)} + 0.65 \cdot \frac{h_i - h_j}{dist_{ij}} \tag{4.11}$$

where n is the number of neighbours, h (m) is tree height, $dist_{ij}$ (m) is the distance between subject tree and competitor, and cr (m) is the mean crown radius. A difference of 1 m in tree height between two trees has the same impact as a decrease of the horizontal distance between those two trees of 1.5 m. The equation is applied for every neighbour and the sum over all competitors is the value of the competition index. A neighbouring tree is only considered as competitor if the calculated value is greater than zero.

Table 4.3: Competition indices for the nine experimental trees. For description see text.

ID	h:dbh	CI_{10}	CI_{11}	CI_{12}	CI_{Hegyi}	$CI_{\text{Schütz}}$
4	49.4	0.55	0.08	0.37	1.85	2.01
37	73.7	0.91	0.13	0.92	3.80	0.66
38	70.1	1.11	0.15	1.26	4.16	2.81
39	75.9	1.07	0.20	1.28	2.61	3.59
40	74.5	0.92	0.18	1.43	3.01	1.91
41	71.6	1.33	0.22	1.75	3.03	5.46
42	79.9	1.51	0.21	2.31	5.65	4.58
43	64.7	0.60	0.11	0.41	1.98	0.14
80	58.6	0.68	0.10	0.48	2.18	0.68

4.2.6 Modified competition index

Wind is a vector and is therefore not just determined by its absolute value but also by direction. Taking this into consideration for the calculation of competition indices means, that the tree position in relation to the wind direction should be taken into consideration. Neighbouring trees, which are located on the leeward side of the subject tree, do not have a sheltering effect on the subject tree. At the same time it seems sensible to weight neighbours which line up with the wind direction higher than those, whose angle deviates from the wind direction. Here the deviation from the wind direction is weighted in an interval from zero to unity for the interval [0:90] degrees using a cosine function.

The mathematical expression for the modified Schütz index looks like:

$$CI_{\text{Schütz}} = \sum_{i=1}^{n} I(wd) \cdot \left(0.5 - \frac{dist_{ij} - (cr_j + cr_i)}{(cr_j + cr_i)} + 0.65 \cdot \frac{h_i - h_j}{dist_{ij}} \right) \tag{4.12}$$

$$I(wd) = \begin{cases} 0 & if \quad |\text{angle} - \text{wd}| \geq 90, \\ cos(angle - wd) & if \quad |\text{angle} - \text{wd}| < 90. \end{cases}$$

where wd (°) is wind direction and $angle$ (°) is the angle between competitor and objective tree. For an illustration see Figure 4.4

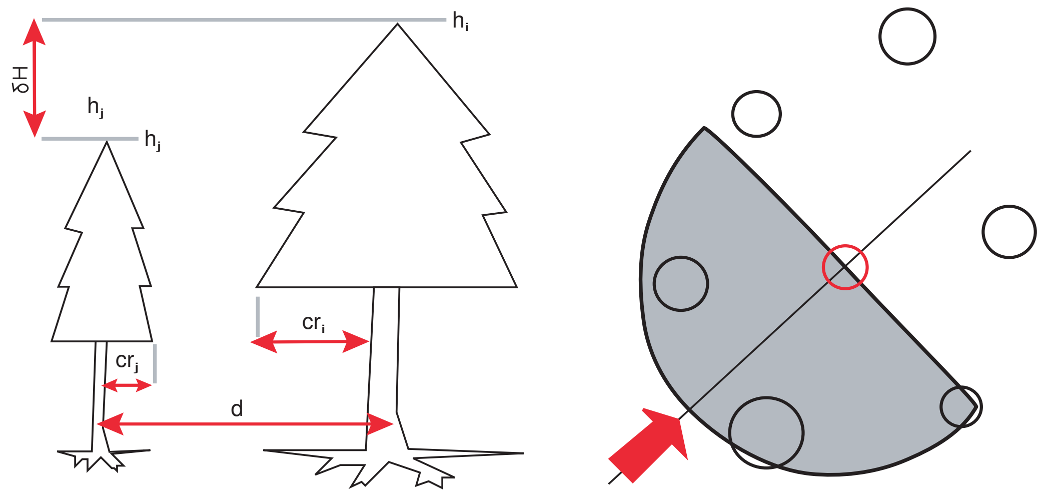

Figure 4.4: Illustration of the Schütz index (left hand side) and schematic explanation of the modified Schütz Index (right hand side). Only trees located within the half circle are considered as neighbours. The red thick arrow in the lower left corner indicates the wind direction.

4.2.7 Thinning scenarios

The maintenance of an irregular stand structure requires regular thinning to create a light regime at the forest floor which encourages the establishment and survival of natural regeneration (Hale, 2003; Hale et al., 2004). For the experimental stand three different thinning scenarios were simulated. For the purpose of comparison the removed basal area is the same for the three scenarios. The basal area, which is removed during one thinning operation is 20 % of the original value (30.8 m^2). The three scenarios differ in the way the harvested trees are selected. In the sections below the three scenarios are briefly described.

From above

The thinning scenario *from above* targets the tallest trees in the stand. All trees are ranked by height and the tallest tree is removed. This is iterated until the target basal area is reached. Neighbours of any harvested tree are preserved from cutting to avoid the creation of bigger gaps. 40 trees need to be harvested to reach the target basal area.

From below

In the *from below* scenario the smallest trees in the stand are removed. As in the scenario *from above* adjacent trees are supposed to remain in the stand. However, due to the smaller diameters of the harvested trees more trees need to be removed and it is not possible to meet the basal area target without removing adjacent trees. This thinning scenario removes 74 trees.

Neutral

The *neutral* scenario has the aim to remove the same percentage of trees in every *dbh*-class (3 cm bin size). Again no adjacent trees were removed. This is the only scenario which contains a certain degree of randomness. The trees are not ranked in any way before the first tree is chosen. For every step only the *dbh*-class is defined from which a tree is chosen. The tree which is harvested from this class is selected randomly after making sure that none of its neighbours has already been removed. The number of trees that is harvested to reach the 20 % target is 60.

For every tree in the stand the critical turning moment is calculated using the formulas, which are implemented in the ForestGALES model (Dunham et al., 2000; Gardiner et al., 2000). The critical turning moment is the lower of the two values breaking and overturning moment. At the same time the competition

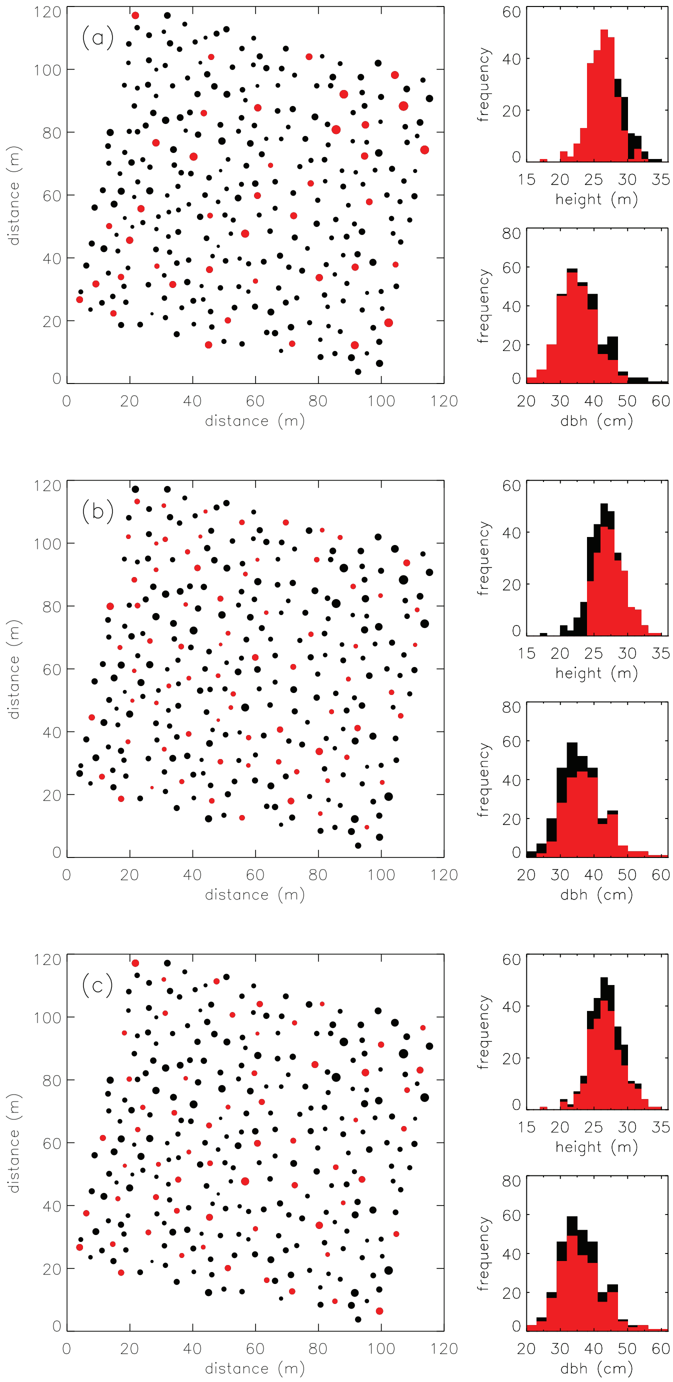

Figure 4.5: Thinning scenarios for the Clocaenog stand (a) from above, (b) from below, and (c) neutral. Circles represent the trees and are scaled by dbh. Red circles represent trees that are harvested. The bar plots on the right hand side are the distributions of height and dbh before (black) and after (red) thinning. The bin size is 1 m and 3 cm, respectively.

indices for all of the trees in the stand are calculated and the critical wind speeds (u_{crit}) are estimated from the relationship between TMC and critical turning moment (M_{crit}), where TMC is calculated as a function of a competition index. The critical wind speed for the trees of the stand are calculated as:

$$u_{crit} = \sqrt{\frac{M_{crit}}{TMC}} \quad \text{where} \quad TMC = f(CI) \tag{4.13}$$

4.3 Results

4.3.1 TMC versus competition indices

In Figure 4.6 the TMCs are plotted against six competition indices. As expected the competition indices are negatively correlated with TMC. All coefficients of correlation (see Tab. 4.4) have a magnitude greater than 0.6 indicating that the indices explain most of the variance. The best data fitting is achieved for the simplest index (*h:dbh*). Because this index is not distant dependent, the removal of an adjacent tree would not cause a change in competition and the regression model would not predict a higher TMC. Therefore we regard the *h:dbh* ratio more as a result of the competition process and adaptive growth of the tree rather than an independent variable itself.

In five of the six plots in Figure 4.6 tree 4 is an outlier. Tree 4 is the most dominant tree in the sample and its measured TMC is in all cases higher than the modelled one. In four out of six cases the correlation coefficients increase when tree 4 is removed from the analysis (see Tab. 4.4).

4.3.2 Impact of wind direction on TMC

The influence of wind direction on the turning moment coefficient is tested for trees 4 and 37. The calculated modified Schütz indices for the two trees show variation, when it is plotted as a function of direction (see Fig. 4.7). Two wind sectors of 40° width were chosen for comparison. The first sector is [240:280] degrees and the second one covers the sector [150:190] degrees. The centres of the two sectors are aligned perpendicularly. Most gale events at the experimental

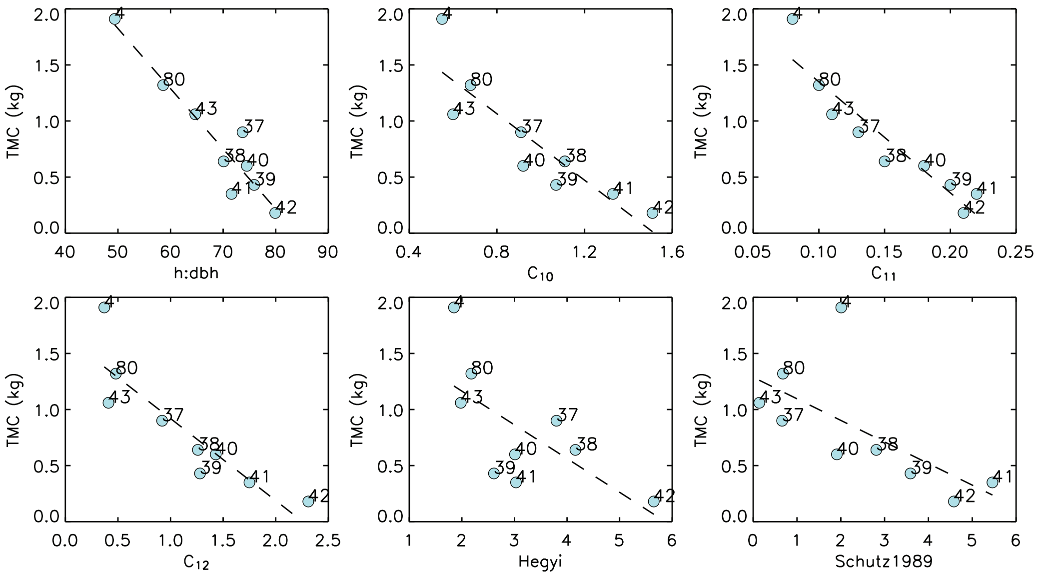

Figure 4.6: Turning moment coefficients (TMC) plotted against the six competition indices. The dashed lines represent the best fit of a linear regression.

site come from a south-westerly to westerly direction, which is also the overall prevailing wind direction. The high values for the southerly sector belong to a single gale event. Due to the lack of gale events from other directions the comparison is limited to these two wind sectors.

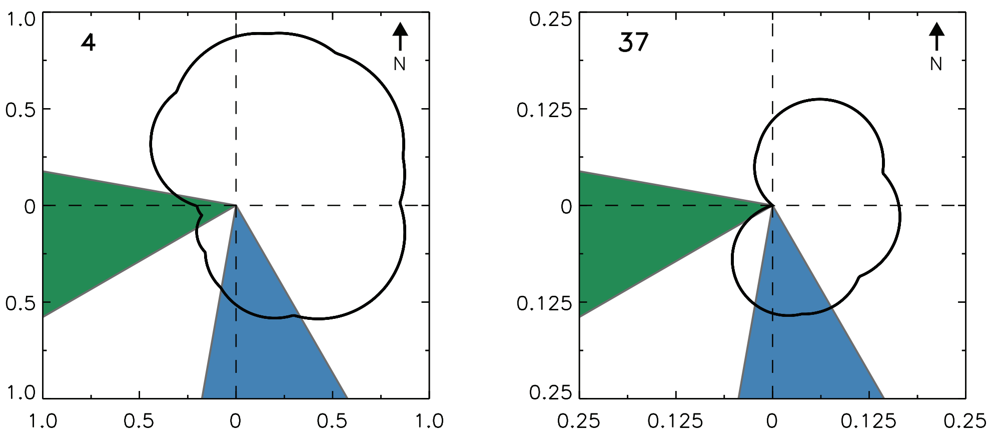

Figure 4.7: Polar plot of the modified Schütz index for tree 4 and tree 37. The green areas represent the wind sector [240:280] and the blue areas the wind sector [150:190] degrees. These are the two sectors, which are used for the regression analysis in Figure 4.8 and Table 4.5.

The sitemap in Figure 4.1 shows gaps in westerly direction for tree 4 and

Table 4.4: Correlation coefficient and root mean square errors (RMSE) for the six plots in Figure 4.6. The coefficients are calculated for data sets *with* and *without* tree 4.

CI	all trees		without ID 4	
	r	RMSE	r	RMSE
h:dbh	-0.95	0.17	-0.88	0.32
CI_{10}	-0.89	0.23	-0.92	0.41
CI_{11}	-0.94	0.18	-0.96	0.37
CI_{12}	-0.89	0.24	-0.94	0.34
CI_{Hegyi}	-0.68	0.38	-0.63	0.34
$CI_{Schütz}$	-0.65	0.39	-0.89	0.40

tree 37. In this direction competition is reduced for both trees as it can be seen in Figure 4.7. Since for the modified Schütz index fewer trees are considered as competitors, the absolute values are lower than the ones in Table 4.3. Two tall neighbouring trees (5: 27.8 m, 6: 27.4 m) result in higher competition for the southerly wind direction compared to the westerly one for tree 4. The neighbours (77: 21.6 m, 79: 28.6 m) in westerly direction of tree 37 are smaller than tree 37, which results in very low competition for this direction.

The analysis of the two data pools results in two different regression lines, which are shown in Figure 4.8. The slopes of the regression lines are for both trees higher if the wind is coming from a westerly direction (green line). If the wind is blowing from a westerly direction the trees experience higher turning moment for the same wind speed compared to the southerly direction (blue line). The results of the regression analysis are summarised in Table 4.5.

4.3.3 Impact of thinning on stability

Crown area data are only available for the nine experimental trees and their direct neighbours. Therefore it was not possible to use either the *Hegyi*-Index or the *Schütz*-Index. As the distant independent index *h:dbh* ratio does not change after a thinning it was also disregarded. Therefore the three indices (C_{10}, C_{11}, C_{12}) from the work of Rouvinen and Kuuluvainen (1997) were used. Only the result of index C_{10} are presented here. This index has been chosen even though it does not have the highest coefficient of correlation. However the differences with C_{11} and C_{12} are not significant and due to the fact that the independent parameters are only used in a linear way makes it less prone to measurement error. All values of u_{crit} for individual trees were then calculated and frequency plots calculated

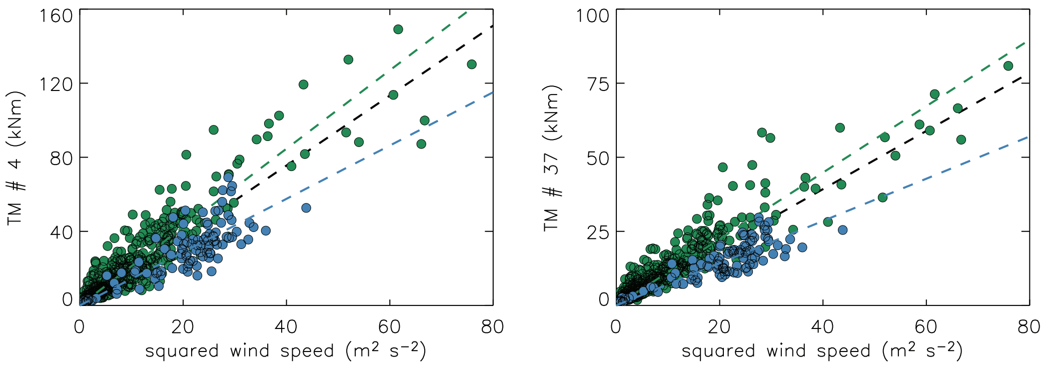

Figure 4.8: Turning moment plotted versus squared wind speed for tree 4 and tree 37. Green data points represent the wind sector [240:280] degrees and blue data points are for the wind sector [150:190] degrees. The green and blue lines represent the best fit of a linear regression for the two different wind sectors, whereas the black line is the best fit for all data points.

of the distribution of all the trees in the plots as a function of the class of critical wind speed. Due to some outliers values between the 10^{th} and 90^{th} percentile are used for analysis.

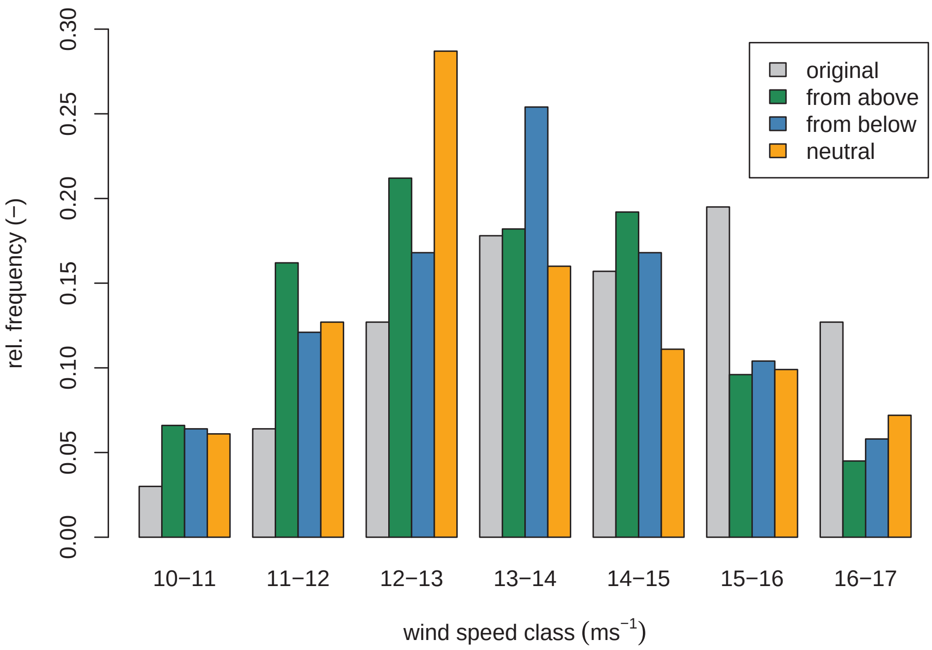

Figure 4.9: Distribution of calculated wind speeds causing tree failure in the range 10–17 $m\,s^{-1}$ for the experimental stand in Clocaenog Forest before and after the application of the thinning scenarios.

Figure 4.9 shows that all three thinning scenarios leave a stand behind which

Table 4.5: Values for the regression analysis in Figure 4.8.

sector	A [240:280] (deg)	B [150:190] (deg)	$A \cup B$ [240:280] ∪ [150:190] (deg)
		Tree 4	
slope (SE)	2.12 (0.031)	1.44 (0.040)	1.89 (0.029)
r	0.91	0.93	0.89
SE	9.75	8.8	10.9
n	441	104	545
		Tree 37	
slope (SE)	1.12 (0.016)	0.71 (0.016)	0.98 (0.015)
r	0.92	0.95	0.89
SE	4.84	3.61	5.68
n	404	102	506

is less stable than the original one. For the original stand the critical wind speed class 15–16 $m\,s^{-1}$ is the one with the highest number of members. The harvesting causes a shift of the median value to lower wind speed classes.

The change in frequency in the wind speed class 10–11 $m\,s^{-1}$ is very similar for all three scenarios. About 3 % more trees are members of this wind speed class after the thinning compared to the stand before the thinning. The superiority of the *from below* scenario can be seen in the two next wind speed classes 11–12 $m\,s^{-1}$ and 12–13 $m\,s^{-1}$. In those two classes the *neutral* and *from above* scenario gain more trees than the *from below* scenario. The *neutral* scenario has the highest gain in the wind speed class 12–13 $m\,s^{-1}$.

The three management scenarios and their influence on the critical wind speed are summarised in Table 4.6. The mean critical wind speeds for the three scenarios are similar. This is to some extend surprising. The reason for this is the fact that almost twice as many trees needs to be harvested for the *from below* scenario compared to the *from above* scenario. Due to the smaller numbers less trees are affected in the *from above* scenario. However, trees that are affected experience a bigger change of the competition index and hence a bigger change in wind loading. Hence the mean values in Table 4.6 give only limited information. The stability of a stand is better defined by its weakest members.

The differences for the *from below* scenario in comparison to the two others would have been more pronounced if no adjacent trees had been harvested. It is believed that a lower target basal area, which could have been achieved without the removal of adjacent trees, would have resulted in more pronounced advantage of this scenario. However, the ranking of the mean critical wind speed is as expected. The *from below* scenario has the highest value, followed up by the *neutral* scenario. The *from above* scenario leaves the stand in the most vulnerable condition.

Table 4.6: Summary of the three thinning scenarios. Total basal area of the stand before thinning was 30.8 m^2. Calculated critical wind speed for the original stand is calculated as 14.6 $m\,s^{-1}$.

	from above	from below	neutral
BA removed (m^2)	6.31	6.17	6.25
BA removed (%)	20.5	20.1	20.3
trees removed	40	74	60
mean u_{crit} ($m\,s^{-1}$)	13.2	13.6	13.4
median u_{crit} ($m\,s^{-1}$)	13.2	13.5	13.0
SD u_{crit}	1.3	1.3	1.5

4.4 Discussion

The correlation coefficients for competition and TMC have all negative values. Lower competition is associated with higher TMCs, i.e. higher turning moment for a certain wind speed. The correlation coefficients for the indices that were used in this work are in the range of -0.63 to -0.96, which indicates that competition is able to explain a lot of the observed variance. The range of indices used suggest that more input data demanding indices do not perform better than simple ones. In fact the most data demanding indices ($CI_{\text{Schütz}}$ and CI_{Hegyi}), which both use crown information, have the lowest correlation coefficients. In this study average crown radius was used as a parameter. Thus irregularities in crown shape are not accounted for and might be an inappropriate simplification. But even an irregularly projected crown shape would not account for the fact that the crown is a three dimensional body. The complexity of the crown shape and the difficulties to measure it makes it an unfavourable and impractical parameter. Detailed and reliable crown information are difficult to collect from the ground without destructive sampling. Remote sensing data might deliver such data in the future but at the moment they are not widely available.

The analysis of two different wind sectors for tree 4 and tree 37 revealed that the TMC is also a function of wind direction. Taking this into consideration requires information about the positions of neighbouring trees in relation to the wind direction. Trees on the leeward site can be neglected, because they do not have any impact on the exposure of the tree. At the same time trees, which are in alignment with the prevailing wind direction, should be weighted more than those which are positioned at an angle from the wind direction. The equations and relationships used here should be considered as a suggestion. The data from this field study are not sufficient for a complete parametrisation.

Low competition in one direction can be caused by gaps. In case of tree 4 an extraction track skirts in westerly direction, which results in lower competition from this direction. This also has an impact on the wind loading and the TMC, which is bigger for the direction with lower competition. The same behaviour was observed for tree 37. Stacey et al. (1994) estimated that "a gap of 15 m (one tree height) doubles the turning moment". Because of their abrupt increase of wind loading for the upwind trees, creating gaps should be avoided by all means.

This is the first time that the turning moments of individual trees have been related to competition indices. Therefore it is not possible to make general conclusions and at the moment the results cannot necessarily be transferred to the conditions of other stands than the experimental one. Since the normal rotation period is less than the age of the Clocaenog stand and because clearfelling was until recently the standard management, the stand structure and the low stand density has to be considered as extraordinary for Britain. Due to the low stand density there is always space between neighbouring tree crowns and therefore it can be assumed that crown clashing is irrelevant for the analysis of the wind and tree interaction in this stand. The sitemap in Figure 4.1 suggests that some of the crowns overlap, but this is an artifact, caused by the projection of the maximum crown radii. A three dimensional view would show that there is always space between the crowns at all heights (see also fisheye photographs in Appendix B). It is known that crown clashing is an efficient way for trees to damp swaying and inhibits the occurrence of otherwise higher turning moments (Milne, 1991; Rudnicki et al., 2003). Hence, such a collective of trees can be much more stable than the individuals themselves would appear to be.

The three thinning scenarios create stands with different stability. The most stable stand is created by the *from below* scenario, followed by the *neutral* scenario and the *from above* scenario. For the calculations of critical wind speeds the assumption is made that the intervention has no impact on the wind profile. This is only true to a certain degree, because the roughness of the underlying surface has an influence on the wind profile. The method used is restricted to thinning regimes that do not remove too much of the projected crown area, which changes the surface roughness, alters the wind profile, and changes turbulence characteristics.

4.5 Conclusions

Current wind risk models are not applicable to irregular stand structures such as occur in low impact management systems. These structured stands require new approaches for calculating wind risk, which take the exposure of individual trees into consideration.

Distant dependant competition indices explain much of the variance when they are used as independent variable to explain individual wind loading on trees. However, it seems as if even small gaps cause a rapid increase of wind loading, which has also been described in other studies (Fraser, 1964; Stacey et al., 1994). The sample size of this experiment is not big enough to parametrise the relationship between gap size and wind loading. More high resolution field data of tree response to wind loading are needed to do that.

The fact that competition indices are widely used in forest modelling and especially the fact that they are implemented in growth simulators is promising. Linking the two model types appear to be straight forward and the tree data from a growth simulator would allow an upscaling to stand level and predictions of wind risk through time as the stand matures.

Acknowledgement

The experimental plot was established by Arne Pommerening and Jens Haufe from the University of Wales, Bangor, who generously made the stand data available, which were used for the simulation of the thinning scenarios.

For erecting and lowering the meteorological mast I fell back on the support from the guys from the technical support unit in Talybont: Carl Foster, Brian Jones, Dai Evans, "Dickie", and Justin Chapbell. Thanks go also to Shaun Mochan, who operated the winch during the mast operations.

Building a reliable logging system from scratch with a tight budget was a big challenge and its realisation would have been impossible without the help from Dave Brooks, John Strachan, and Jim Nicholl from the workshop at the Northern Research Station. Their support is much appreciated.

References

Achim A, Ruel JC, and Gardiner BA, 2005: Evaluating the effect of precommercial thinning on the resistance of balsam fir to windthrow through experimentation, modelling, and development of simple indices. *Canadian Journal of Forest Research*, 35, 1844–1853.

Aurenhammer F and Klein R, 2000: *Voronoi Diagrams*, chap. Handbook of Computational Geometry, pp. 201–290. North-Holland, Amsterdam, Netherlands.

Blackburn GRA, 1997: *The Growth and Mechanical Response of Trees to Wind Loading*. PhD, University of Manchester.

Courbaud B, Goreaud F, Dreyfus P, and Bonnet F, 2001: Evaluating thinning strategies using a tree distance dependent growth model: Some examples based on the CAPSIS software "uneven-aged Spruce forests" module. *Forest Ecology and Management*, 145, 15–28.

Dunham R, Gardiner B, Quine C, and Suárez J, 2000: *ForestGALES - A PC-based wind risk model for British forests*. Forestry Commission, Edinburgh, UK.

Fraser AI, 1964: Wind tunnel and other related studies on coniferous trees and tree crops. *Scottish Forestry*, 18, 84–92.

Gardiner B, Peltola H, and Kellomäki S, 2000: Comparison of two models for predicting the critical wind speeds required to damage coniferous trees. *Ecological Modelling*, 129, 1–23.

Hale SE, 2003: The effect of thinning intensity on the below-canopy light environment in a Sitka spruce plantation. *Forest Ecology and Management*, 179, 341–349.

Hale SE, Levy PE, and Gardiner BA, 2004: Trade-offs between seedling growth, thinning and stand stability in Sitka spruce stands: A modelling analysis. *Forest Ecology and Management*, 187, 105–115.

Hegyi F, 1974: A simulation model for managing jack-pine stands. In Fries J, ed., *Growth Models for Tree and Stand Simulation*, pp. 74–90. Royal College of Forestry, Stockholm.

Kenk G and Guehne S, 2001: Management of transformation in central Europe. *Forest Ecology and Management*, 151, 107–119.

Mailly D, Turbis S, and Pothier D, 2003: Predicting basal area increment in a spatially explicit, individual tree model: A test of competition measures with black spruce. *Canadian Journal of Forest Research*, 33, 435–443.

Mason WL, 2002: Are irregular stands more windfirm? *Forestry*, 75, 347–355.

Mayhead GJ, 1973: Some drag coefficients for British forest trees derived from wind-tunnel studies. *Agricultural Meteorology*, 12, 123–130.

Milne R, 1991: Dynamics of swaying of *Picea sitchensis*. *Tree Physiology*, 9, 383–399.

Moore JR, Gardiner BA, Blackburn GRA, Brickman A, and Maguire DA, 2005: An inexpensive instrument to measure the dynamic response of standing trees to wind loading. *Agricultural and Forest Meteorology*, 132, 78–83.

Moore JR and Maguire DA, 2004: Natural sway frequencies and damping ratios of trees: Concepts, review and synthesis of previous studies. *Trees*, 18, 195–203.

Nicoll B and Ray D, 1996: Adaptive growth of tree root systems in response to wind action and site conditions. *Tree Physiology*, 16, 891–898.

Page L, Cameron AD, and Clarke GC, 2001: Influence of overstorey basal area on density and growth of advance regeneration of Sitka spruce in variably thinned stands. *Forest Ecology and Management*, 151, 25–35.

Pretzsch H, Biber P, and Ďurský J, 2002: The single tree-based stand simulator SILVA: Construction, application and evaluation. *Forest Ecology and Management*, 162, 3–21.

Rojo JMT and Orois SS, 2005: A decision support system for optimizing the conversion of rotation forest stands to continuous cover forest stands. *Forest Ecology and Management*, 207, 109–120.

Rouvinen S and Kuuluvainen T, 1997: Structure and asymmetry of tree crowns in relation to local competition in a natural mature Scots pine forest. *Canadian Journal of Forest Research*, 27, 890–902.

Rudnicki M, Lieffers VJ, and Silins U, 2003: Stand structure governs the crown collisions of lodgepole pine. *Canadian Journal of Forest Research*, 33, 1238–1244.

Rudnicki M, Meyer TH, Lieffers VJ, Silins U, and Webb VA, 2008: The periodic motion of lodgepole pine trees as affected by collisions with neighbors. *Trees*, 22, 475–482.

Rudnicki M, Mitchell SJ, and Novak MD, 2004: Wind tunnel measurements of crown streamlining and drag relationships for three conifer species. *Canadian Journal of Forest Research*, 34, 666–676.

Schröder J, Röhle H, Gerold D, and Münder K, 2007: Modeling individual-tree growth in stands under forest conversion in East Germany. *European Journal of Forest Research*, 126, 459–472.

Schütz JP, 1989: Zum Problem der Konkurrenz in Mischbeständen. *Schweizerische Zeitschrift für Forstwesen*, 140, 1069–1083.

Schütz JP, 2001: Opportunities and strategies of transforming regular forests to irregular forests. *Forest Ecology and Management*, 151, 87–94.

Stacey GR, Belcher RE, Wood CJ, and Gardiner BA, 1994: Wind flows and forces in a model spruce forest. *Boundary-Layer Meteorology*, 69, 311–334.

Stadt KJ, Huston C, Coates KD, Feng Z, Dale MR, and Lieffers VJ, 2007: Evaluation of competition and light estimation indices for predicting diameter growth in mature boreal mixed forests. *Annals of Forest Science*, 64, 477–490.

Wonn HT and O'Hara KL, 2001: Height:Diameter ratios and stability relationships for four northern Rocky Mountain tree species. *Western Journal of Applied Forestry*, 16, 87–94.